Catalysis Today 164 (2011) 538–543

Contents lists available at ScienceDirect

Catalysis Today

journal homepage: www.elsevier.com/locate/cattod

Catalyst development for ultra-deep hydrodesulfurization (HDS) of dibenzothiophenes. I: Effects of Ni promotion in molybdenum-based catalysts☆

Qiang Gao, Thomas N.K. Ofosu, Shu-Guo Ma, Vasileios G. Komvokis, Christopher T. Williams, Koichi Segawa*

Department of Chemical Engineering, University of South Carolina, Columbia, SC 29208-4101, United States

ARTICLE INFO

Article history:
Available online 5 November 2010

Keywords:
Hydrodesulfurization (HDS)
Ni promoter
MoS_2 catalyst
Dibenzothiophene (DBT)
X-ray photoelectron spectroscopy (XPS)

ABSTRACT

A strong synergistic effect of nickel and molybdenum was observed for hydrodesulfurization (HDS) of dibenzothiophene (DBT), 4-methyldibenzothiophene (4-MDBT) and 4,6-dimethyldibenzothiophene (4,6-DMDBT) over highly active Ni-MoS_2/γ-Al_2O_3 catalysts. The surface of the most active catalyst in this study was composed by Ni:Mo = 1:3, which was determined by XPS results. In addition, catalytic behavior indicates the presence of two different adsorption models accounting for the DDS (direct desulfurization) and the HYD (hydrogenation) pathways. The structure of the NiMoS active phase appears to be identical regardless of Ni/(Ni + Mo) ratio. The reaction sequence of the DDS pathways is DBT > 4-MDBT > 4,6-DMDBT due to the steric hindrance of methyl groups located adjacent to the sulfur atom of DBT, which prevents σ-bonding of the sulfur to the active site within the NiMoS phase. The reaction rates of HYD pathways are independent of the number of methyl groups, suggesting that the alkyl groups do not interfere the π-adsorption of DBTs on the active sites.

1. Introduction

According to the very strict environmental regulations, the sulfur content of diesel fuel should already have become less than 10 ppm [1–4]. However, it is still necessary to keep the focus on the end goal: sulfur-free transportation fuels (including gasoline, diesel fuels and jet fuels) and non-road fuel. Even though 10 ppm sulfur levels have already been reached in most industrialized countries, more efficient catalysts are still needed to lower the reaction temperature and to reduce the hydrogen consumption by decreasing the hydrogen pressure. Therefore, researchers have a very strong motivation to develop the next generation of highly active HDS catalysts.

For ultra-deep HDS [5–12], it is already known that the most refractory sulfur-containing compounds in gas oil are the alkyldibenzothiophenes (alkyl-DBT). This is especially the case for those substituted in the 4 and 6 positions of the phenyl rings adjacent to the thiophenic one, such as 4,6-dimethyldibenzothiophene (4,6-DMDBT). However, substitution in the other positions has minor effects on the reactivity. Up to now, it has been widely accepted that the HDS of these refractory alkyl-DBT derivatives proceeds through two parallel reaction routes [6–8], as shown in Scheme 1. The first pathway is a direct desulfurization (DDS) pathway that produces dimethylbiphenyl (DMBP). The second pathway involves prehydrogenation (HYD) of one aromatic ring, followed by sulfur removal that produces methyl cyclohexyltoluene (MCHT).

Optimization of hydrodesulfurization (HDS) catalysts is the most appropriate approach to produce the ultra-clean diesel fuel in order to minimize the capital investment and lower operating cost. Supported molybdenum sulfide catalysts [6,7] have been widely used in industrial HDS processes during the last few decades. Regarding the surface structure of such catalysts, Topsøe et al. first proposed the so-called "CoMoS" model [13], indicating some possible locations of Co at the different MoS_2 edge planes. That suggests a possible effect of the morphology of MoS_2 on activity and selectivity, and could explain the results of numerous studies dealing with the structure–function relationship of these systems. In addition, Koningsberger and coworkers classified this model as CoMoS Type I (single slab) and Type II (multilayer slabs) phases [14]. This model has been extended to NiMo catalysts and to HDN reactions. Molybdenum-based catalysts have been characterized with various techniques including extended X-ray absorption fine structure (EXAFS) spectroscopy [15–17], infrared spectroscopy of NO adsorption [18–20], transmission electron microscopy (TEM) [21–23], X-ray photoelectron spectroscopy (XPS) [24], and ^{57}Co Mossbauer emission spectroscopy [6]. Furthermore, the effects of the support in molybdena catalysts were studied intensively over

☆ Student Award Paper.

* Corresponding author at: Department of Chemical Engineering, University of South Carolina, 301 S Main ST, Room 2B22, Columbia, SC 29208-4101, United States. Tel.: +803 777 4693; fax: +1 803 777 8265.
E-mail address: kohichi@cec.sc.edu (K. Segawa).

0920-5861/$ – see front matter © 2010 Elsevier B.V. All rights reserved.
doi:10.1016/j.cattod.2010.10.016

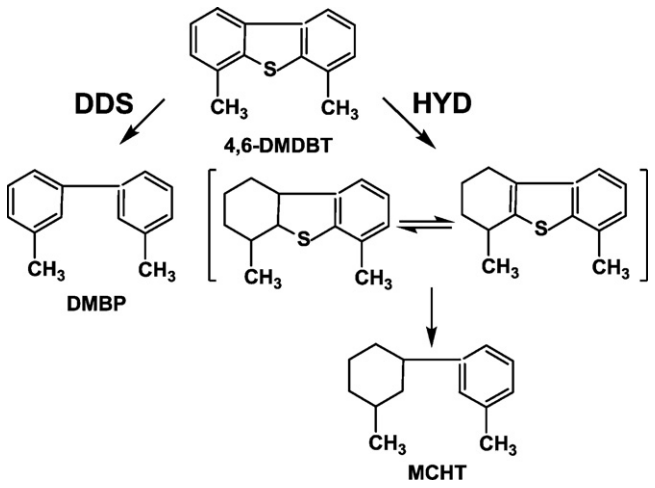

Scheme 1. Reaction pathways for the HDS of 4,6-dimethyldibenzothiophene (4,6-DMDBT).

the past decade. For example, Segawa and co-workers [25–31] published a group of papers for HDS of DBT derivatives over Ni-MoS_2 catalysts supported on TiO_2–Al_2O_3 and B_2O_3–Al_2O_3 support.

Notwithstanding the number of studies already available in the literature, several issues are still open questions, including whether the DDS and HYD pathways occur at the same or at different active sites, what is the key factor for determining the pathway selectivity, and which synthetic methodology will allow design and preparation of the most active HDS catalyst. In this paper we report the synergistic effects of the addition of nickel promoter in conventionally prepared Ni-MoS_2/γ-Al_2O_3 catalyst for the HDS of DBT, 4-MDBT and 4,6-DMDBT. Our major goal is to correlate the HDS catalytic activity with the surface atomic composition and especially the NiMo ratio by combining kinetic studies with XPS characterization. Furthermore, we will try to define the relation between the catalytic activity and selectivity with the reactants (DBT, 4-MDBT and 4,6-DMDBT), as well as whether the reaction pathways (DDS or HYD) proceed via different active sites.

2. Experimental

2.1. Preparation of catalyst

Highly active Ni-MoS_2/γ-Al_2O_3 catalysts with various Ni/(Ni + Mo) atomic ratios were prepared by a standard co-impregnation method [32]. A 5 g aliquot portion of porous γ-Al_2O_3 support (BET surface area 279 m^2/g, pore volume 0.59 cc/g) was impregnated with an aqueous solution of ammonium heptamolybdate $(NH_4)_6Mo_7O_{24}{\cdot}4H_2O$ (Fluka, >99%) and nickel nitrate $Ni(NO_3)_2{\cdot}6H_2O$ (Aldrich, 99.999%). The amounts of ammonium heptamolybdate and nickel nitrate were adjusted in order to reach 15 wt% ($NiO + MoO_3$) loading. The Ni/(Ni + Mo) ratio was varied from 0 to 1. The obtained solid was dried at 100 °C for 10 h, and then calcined at 500 °C for 10 h under ambient condition. Prior to HDS reaction, the catalyst was activated *in situ* by sulfiding treatment to obtain active Ni-MoS_2/γ-Al_2O_3 catalysts.

2.2. HDS catalytic reactions

The HDS reactions over Ni-MoS_2/γ-Al_2O_3 catalysts were carried out in a fixed bed high pressure reaction system under plug-flow condition. The reactor consists of a 1.27 cm outer diameter/0.97 cm inner diameter, 45 cm long stainless steel tubular reactor with an aluminum cylindrical surrounding block (2.54 cm diameter and 38 cm length). The powder catalyst (25–300 mg, 100 mesh) was diluted with 0.5 g silica gel (Sigma–Aldrich, Davisil, Grade 636, pore size 60 Å, 36–60 mesh), and then the mixture was placed in the center of the reactor, sandwiched with inert layers (Norton, Denstone 57, 1/8 in.). DBT (Aldrich, 99%), 4-MDBT (Sigma–Aldrich, 96%) and 4,6-DMDBT (Aldrich, 97%) were diluted with n-hexadecane (Sigma–Aldrich, 99.8%) and toluene (Sigma–Aldrich, 99%) at the molar ratio of 1:8:130 in order to reach 2000 ppm sulfur concentration. The DBT liquid reagents were charged by the high pressure liquid feed pump (TELEDYNE ISCO, 260D).

Before starting HDS reactions, samples were heated from room temperature to 400 °C with a constant temperature increase (3 °C min^{-1}) and then held for 10 h, while flowing H_2S/H_2 (5% H_2S) at 30 cm^3 min^{-1} under atmospheric pressure. After that, the reactor was cooled down to the desired reaction temperature (270–310 °C) under a constant pressure of H_2 (3 MPa). Finally, the liquid reagent was fed to the reactor by means of the high-pressure liquid pump (feed rate: 2–60 ml/h as needed).

The HDS catalytic tests were conducted at a constant pressure (3 MPa) with a constant H_2 flow rate at 200 cm^3 min^{-1}, and a LHSV (liquid hourly space velocity) ranging from 300 to 3600 h^{-1}. The conversion level was kept at below 20% and the selectivity was calculated at 10% conversion. The liquid products were collected from a gas–liquid separator and then directly analyzed with a HP5890 II GC equipped with FID and a capillary column (DB-5). GC–MS (mass spectrometry, VG-70S mass spectrometer) was used to identify the observed reaction products. The temperature in the oven of GC was heated from 175 °C to 300 °C with the ramp of 10 °C min^{-1} and held at 300 °C for 2.5 min in order to separate the reaction products.

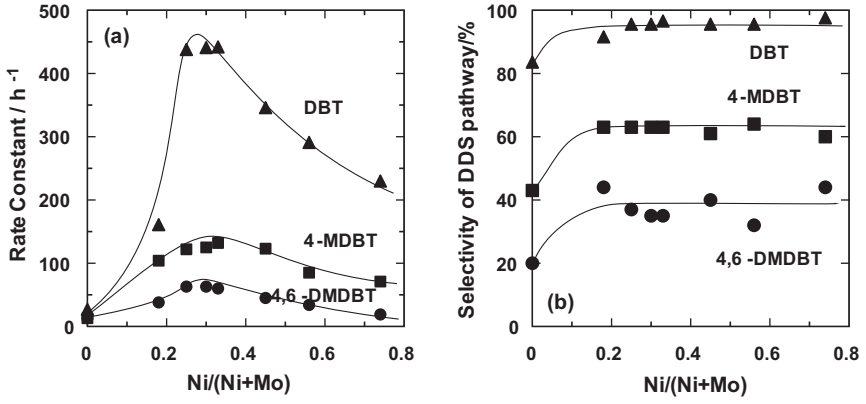

Fig. 1. Catalytic activities (a) and DDS selectivities (b) for HDS of DBTs over Ni-MoS_2/γ-Al_2O_3 catalysts. Selectivity was determined at 10% conversion. Reaction conditions: 2000 ppm sulfur, 3 MPa, 310 °C, LHSV = 300–3600 h^{-1}, H_2 flow rate = 200 cm^3 min^{-1}.

2.3. Characterization with X-ray photoelectron spectroscopy (XPS)

XPS was employed to specify the states of nickel and molybdenum present before and after sulfidation treatment. Measurements were conducted on a Kratos AXIS Ultra DLD XPS system equipped with a hemispherical energy analyzer and a monochromatic Al Kα source (486.6 eV), which was operated at 15 keV and 150 W, incident at 45° with respect to the normal surface. The pass energy was fixed at 40 eV for the detailed scans. A charge neutralizer was used to compensate for the surface charge, since the sample was nonconductive.

Oxidized samples were evacuated down to 1.33×10^{-7} Pa at room temperature for measurement in the XPS preparation chamber. The sulfided samples can be obtained by *ex-situ* sulfiding treatment of oxidized catalysts at 400 °C under H_2S/H_2 flow (5% H_2S) for 3 h at atmospheric pressure. Those sulfided samples were then placed in the preparation chamber and treated with H_2 flow at 380 °C for 1 h, followed by transfer into the main chamber without exposure to air. Finally, samples were evacuated to 1.33×10^{-7} Pa before XPS measurement.

All spectra were corrected using 71.33 eV as a reference for Al2p binding energy (BE). The spectra were fitted to a Shirley-Linear background using XPSPEAK software version 41. The deconvolution was accomplished with Gaussian-Lorentzian band shapes. Several constraints for the deconvolution of Mo3d peaks were considered: (1) the theoretical spin-orbit splitting of the Mo3d peaks was 3.13 eV; (2) the ratio of peak area between $Mo3d_{5/2}$ and $Mo3d_{3/2}$ was kept constant at 3:2; (3) the full width at half maximum (FWHM) values of the $Mo3d_{5/2}$ and $Mo3d_{3/2}$ peaks were assumed to be identical. In the case of Ni2p, these parameters of $Ni^{2+}2p_{3/2}$ and $Ni^{2+}2p_{1/2}$ are: (1) 17.49 eV; (2) 2; (3) identical.

3. Results and discussion

3.1. HDS catalytic reaction

Kinetic evaluations for HDS of DBT, 4-MDBT and 4,6-DMDBT were performed at a constant H_2 pressure (3 MPa) in the temperature range of 270–310 °C over active NiMo/γ-Al_2O_3 catalysts with different Ni/(Ni + Mo) atomic ratios. Figure 1 shows the overall rate constants (a) and selectivities (b) for HDS of DBT, 4-MDBT and 4,6-DMDBT. In Fig. 1(a), it can be seen that the HDS activity of DBT over MoS_2/γ-Al_2O_3 is greatly enhanced with the addition of Ni. This phenomenon can also be observed in the cases of HDS of 4-MDBT and 4,6-DMDBT. Furthermore, the pseudo-first order rate constant goes through a maximum for Ni/(Ni + Mo) bulk atomic ratio of around 0.33, where the value is approximately 20 times higher than that of Mo alone. In the region beyond Ni/(Ni + Mo) = 0.33, the activity starts to decline significantly. Similar plots for HDS of 4-MDBT (squares) and 4,6-DMDBT (circles) are obtained for the same family of catalysts. In both plots, the maximum is again observed for the Ni/(Ni + Mo) bulk atomic ratio of around 0.33. This indicates that the maximum number of active sites is present in the catalysts with Ni/(Ni + Mo) ratios of about 0.33. In addition, the rate constants are decreased by roughly a factor of 2-3 in the case of 4-MDBT, and yet another two fold in the case of 4,6-DMDBT over the whole range with different Ni/(Ni + Mo) ratios. This confirms that the HDS activity decreases following in the order: DBT > 4-MDBT > 4,6-DMDBT. Prins and coworkers [33] also found that the Ni promoter increased the rates in the reaction network of DBT and 4,6-DMDBT, especially the direct desulfurization steps.

As shown in Fig. 1(b), the selectivity of the DDS pathway is significantly enhanced upon addition of Ni to molybdenum catalysts for the HDS of all three DBT derivatives. This suggests that the presence of nickel favors the DDS pathway (i.e., hydrogenolysis), and thus is contributing to the formation of the catalytic active phase. Moreover, it is notable that the DDS selectivities for HDS of DBTs over all bimetallic Ni–Mo catalysts remained almost constant regardless of Ni/(Ni + Mo) atomic ratio, although the activity is greatly influenced by Ni content. These results suggest that the catalytic property of the highly active sites is identical regardless of Ni/(Ni + Mo) ratio. Additionally, the significant decreases in catalytic activity for the HDS of 4-MDBT and 4,6-DMDBT as compared to DBT, is accompanied by a declines in the DDS selectivity.

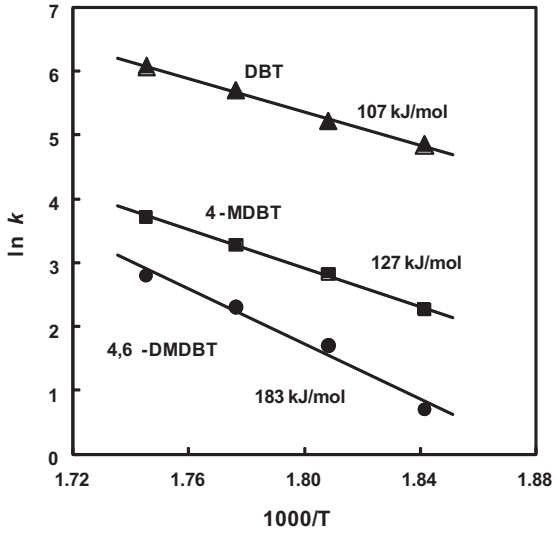

Fig. 2. Arrhenius plots for HDS of DBTs over Ni-MoS_2/γ-Al_2O_3 catalyst with Ni/(Ni + Mo) = 0.33. Reaction conditions: 2000 ppm sulfur, 3 MPa, 270–300 °C, LHSV = 300–3600 h^{-1}, H_2 flow rate = 200 cm^3 min^{-1}.

In order to evaluate the activation energy, we adjusted the temperature within the range of 270–300 °C. Fig. 2 shows the Arrhenius plots for HDS of DBT, 4-MDBT and 4,6-DMDBT over the Ni-MoS_2/γ-Al_2O_3 catalyst with the Ni/(Ni + Mo) ratio of 0.33. Apparent activation energies were 107 kJ/mol for DBT, 127 kJ/mol for 4-MDBT and 183 kJ/mol for 4,6-DMDBT. It can be seen that the activation energy increases with the increase of the number of methyl groups located near the sulfur atom of the DBT molecule. Thus, the methyl groups appeared to inhibit the C–S bond scission of the adsorbed DBTs on the active sites. It is notable to mention that the selectivity of the DDS pathway is almost unchanged within the temperature range of this study (270–310 °C). Moreover, the activation energy obtained in this study (above 80 kJ/mol) indicates that the reaction is not limited by diffusion in the bulk phases. This is similar to the research results from Kabe and co-workers [34], who pointed out that the values of activation energies of HDS reflect the relative difficulty of desulfurization of DBTs. They also reported that 4-MDBT and 4,6-DMDBT are adsorbed on the catalyst more strongly than DBT.

Table 1 summarizes the pseudo-first order rate constants *k* for DDS and HYD pathways, as well as the activation energies for HDS

Table 1
Summary of rate constants and activation energies for HDS of DBTs over Ni-MoS_2/γ-Al_2O_3 catalyst.

Reactant	k_{TOTAL} (h^{-1})	k_{DDS} (h^{-1})	k_{HYD} (h^{-1})	Ea (kJ/mol)
DBT	438	402	36	107
4-MDBT	131	90	41	127
4,6-DMDBT	63	26	37	183

Reaction conditions: Ni/(Ni + Mo) = 0.33, 2000 ppm sulfur, 3 MPa, 270–300 °C, rate constant *k* was determined at 310 °C, LHSV = 300–3600 h^{-1}, H_2 flow rate = 200 cm^3 min^{-1}.

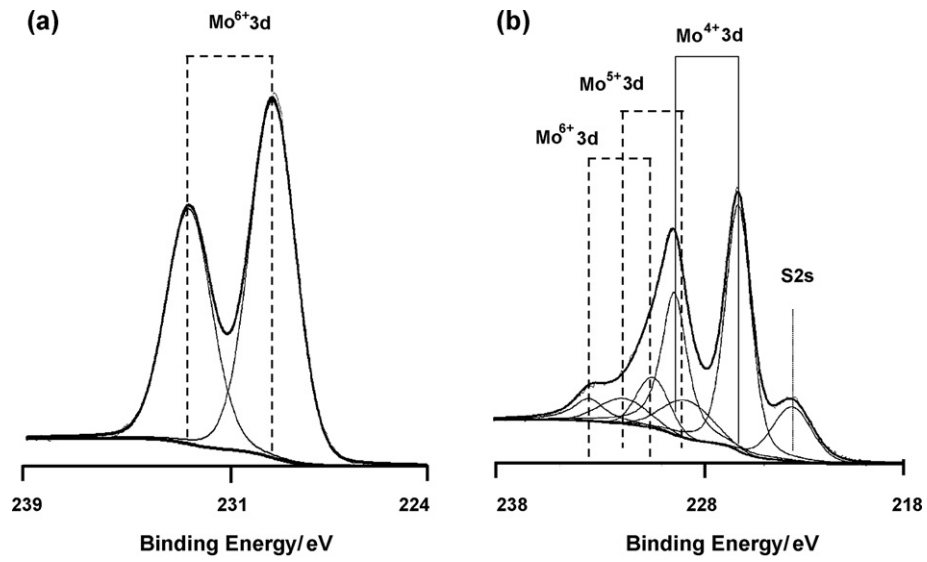

Fig. 3. Mo3d XPS spectra of Ni–Mo/γ-Al_2O_3 catalyst with Ni/(Ni + Mo) = 0.33 before (a) and after (b) sulfiding treatment. Binding energy: $Mo^{6+}3d_{3/2}$ = 232.88 eV, $Mo^{6+}3d_{5/2}$ = 229.75 eV, $Mo^{4+}3d_{3/2}$ = 228.73 eV, $Mo^{4+}3d_{5/2}$ = 225.60 eV, S_{2S} = 222.72 eV.

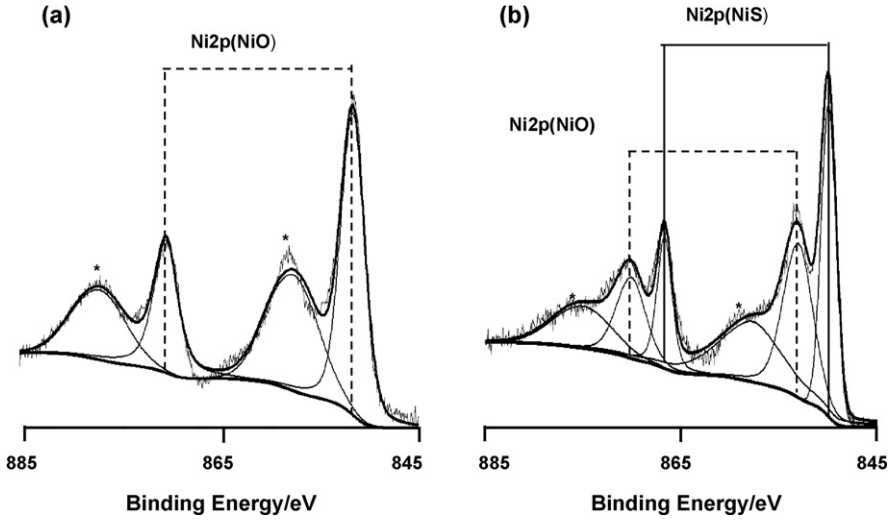

Fig. 4. Ni2p XPS spectra of Ni–Mo/γ-Al_2O_3 catalyst with Ni/(Ni + Mo) = 0.33 before (a) and after (b) sulfiding treatment. Binding energy: (a) $Ni^{2+}2p_{1/2}$ = 871.05 eV, $Ni^{2+}2p_{3/2}$ = 853.41 eV and (b) $Ni^{2+}2p_{1/2}$ = 867.27 eV, $Ni^{2+}2p_{3/2}$ = 850.07 eV, *satellite peak.

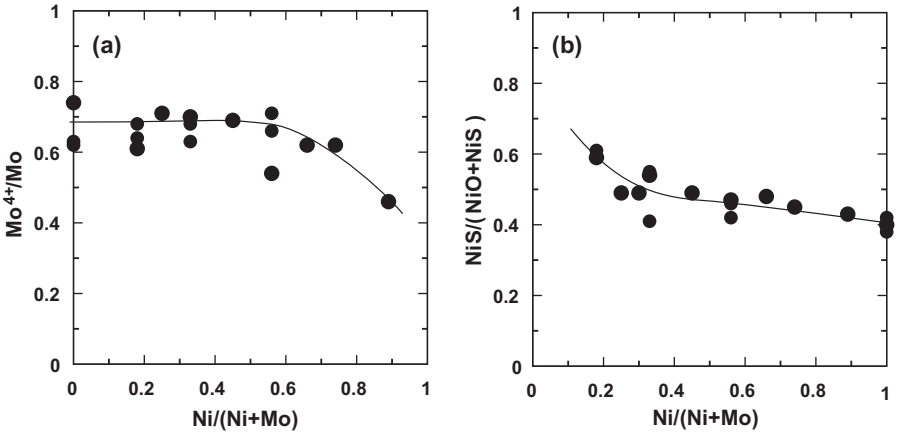

Fig. 5. The sulfidation degree of Mo (a) and Ni (b) as a function of Ni loading over Ni-MoS_2/γ-Al_2O_3 catalysts.

of DBT, 4-MDBT and 4,6-DMDBT obtained from the catalyst consisting a Ni/(Ni + Mo) ratio of 0.33. Each of these rate constants (k_{DDS} and k_{HYD}) was calculated by multiplying the overall HDS rate constant by its associated DDS and HYD selectivity. The changes in activity and selectivity observed with different catalysts can largely be understood in terms of an alteration in the ability of the catalyst to facilitate the DDS reaction pathway (see Scheme 1). It can be seen that the rate constant for the DDS pathway is extremely retarded by the presence of methyl groups adjacent to sulfur atom in dibenzothiophenes in the order of DBT > 4-MDBT > 4,6-DMDBT. This phenomenon is very likely to occur due to steric hindrance generated by methyl substitution near the sulfur atom.

On the other hand, the HDS rates of the HYD pathway were essentially independent of the number of methyl groups, and thus apparently not related to steric hindrance. For instance, in Table 1 the rate constants of the HYD reaction pathway are 36 h^{-1} for DBT, 41 h^{-1} for 4-MDBT, and 37 h^{-1} for 4,6-DMDBT. These results may suggest that the DDS and HYD reaction pathways might occur at different types of adsorption sites on the Ni-MoS_2/γ-Al_2O_3 catalyst.

It is relatively straightforward to understand why there is a significant steric hindrance in 4,6-DMDBT as compared to DBT, if one compares their conformations. It can be seen that the sulfur atom in DBT is accessible for bonding, allowing DBT to adsorb on an active site via a sulfur–metal interaction (σ-bonding). However, in the case of 4,6-DMDBT, the two methyl groups at the 4- and 6-positions inhibit the interaction of the sulfur atom with the active site via a sulfur–metal bond. Therefore, 4,6-DMDBT preferentially undergoes π-complexation (π-bonding) rather than sulfur–metal interactions (σ-bonding) on the active site, which favors the HYD instead of the DDS reaction pathway [35]. In addition, Segawa and coworkers [36] proposed a flat adsorption mechanism of 4,6-DMDBT via the HYD route, for which steric hindrance could be avoided.

3.2. Characterization of NiMo/γ-Al_2O_3 catalysts by XPS

Information on elemental composition and the oxidation state of the metals can be provided by XPS measurements. Thus, the states of NiMo species before and after sulfiding treatment were investigated. XPS spectra of Mo3d and Ni2p over the most active Ni–Mo/γ-Al_2O_3 catalyst with Ni/(Ni + Mo) = 0.33 before (a) and after (b) sulfiding treatment are shown in Figs. 3 and 4, respectively. As can be seen, the samples before sulfiding are oxidized in the Mo^{6+} and Ni^{2+} states. Upon sulfiding, the majority of the Mo^{6+} converts to Mo^{4+}, while the formation of nickel sulfide species can be identified. However, neither Mo nor Ni can be sulfided completely. Some unsulfided species of Mo^{6+} and Ni^{2+} still remain on the surface, which can associate with oxygen atoms. The Mo^{5+} species and expected S_{2S} occur after sulfiding; identical conclusions also proposed by Niemantsverdriet [37] during a study of the sulfidation mechanism of MoO_3.

As shown in Fig. 5(a), the Mo^{4+}/Mo ratio is a function of Ni atomic composition. The repeatable data indicate us that the Mo^{4+}/Mo ratio is almost constant at around 0.65 in the Ni/(Ni + Mo) ratio range of 0–0.7. Meanwhile, some unsulfided Mo^{6+} surface species still exist even after extensive sulfiding treatment. It is notable that the surface appears slightly enriched in Mo in the oxidized state. However, Mo segregation on the surface is enhanced after sulfiding.

Fig. 5(b) represents the NiS/(NiS + NiO) ratio as a function of Ni loading over Ni-MoS_2/γ-Al_2O_3 catalysts. As it can be seen, the NiS/(NiS + NiO) ratios are decreasing gradually from 0.6 to 0.4. Since NiS species contribute to the NiMoS active phase, it would be much better if the NiS/(NiS + NiO) ratio could be increased to a higher level. However, some other Ni species is possible to be formed on the surface, which can further associate with oxygen atoms, leading to the formation of aluminate species. Moreover, Eijsbouts *et al.* found the formation of some large Ni_3S_2 bulk particles in commercial Ni–Mo catalysts [38]. In addition, there is significant Ni sulfide segregation in commercial Ni–Mo catalysts, although they have high MoS_2 dispersion.

According to the sulfidation degree, the calculated surface atomic ratio is about Ni:Mo = 1:3 for the catalyst at Ni/(Ni + Mo) = 0.33. That means the Ni:Mo ratio changes from 1:2 in the bulk phase (in the oxidized state) to 1:3 on the surface phase (in the sulfided state) after sulfiding treatment.

4. Conclusions

A strong synergistic effect of nickel and molybdenum was observed with the addition of Ni over MoS_2/γ-Al_2O_3 catalysts for HDS of DBT, 4-MDBT and 4,6-DMDBT at 3 MPa within the temperature range from 270 to 310 °C. Ni promoter enhances the selectivity of DDS pathway compared to monometallic MoS_2/γ-Al_2O_3 catalyst, while the HYD selectivities over all Ni-MoS_2/γ-Al_2O_3 catalysts remain almost constant and independent of Ni/(Ni + Mo) atomic ratios. The structure of NiMoS active phase thus appears to be identical regardless of the Ni/(Ni + Mo) ratio. The maximum catalytic activity for the HDS of DBT derivatives can be found at a Ni/(Ni + Mo) bulk atomic ratio of around 0.33. According to the sulfidation degree, activity of catalysts as a function of the atomic composition suggests that a roughly 1:3 surface Ni:Mo ratio (1:2 in the bulk phase) produces the most active NiMoS site, and most likely the largest number of them.

In addition, catalytic behavior as a function of the reactants suggests that the DDS and HYD reaction pathway might occur at different type of adsorption site on the Ni-MoS_2/γ-Al_2O_3 catalyst. The reaction sequence of the DDS pathway is DBT > 4-MDBT > 4,6-DMDBT due to the steric hindrance of methyl groups located near the sulfur atom of DBT which prevents σ-bonding of the sulfur to the active site within the NiMoS phase. The reaction rates of HYD pathway are independent of the number of methyl groups at 4 and 6 position of DBT molecule, thus suggesting that the alkyl groups do not hinder the π-adsorption of DBTs on the active sites in the NiMoS phase.

Acknowledgements

The financial support from UOP LLC, a Honeywell company is greatly acknowledged. Additional support from the USC Nanocenter is also greatly appreciated.

References

[1] J.R. Rostrup-Nielsen, Catal. Rev. Sci. Eng. 46 (2004) 247.
[2] I.V. Babich, J.A. Moulijn, Fuel 82 (2003) 607.
[3] H. Topsøe, B. Heinemann, J.K. Norskov, J.V. Lauritsen, F. Besenbacher, P.L. Hansen, G. Hytoft, R.G. Egeberg, K.G. Knudsen, Catal. Today 107 (2005) 12.
[4] C. Song, Catal. Today 86 (2003) 211.
[5] A. Stanislaus, B.H. Cooper, Catal. Rev. Sci. Eng. 36 (1994) 75.
[6] H. Topsøe, B.S. Clausen, F.E. Massoth, in: J.R. Anderson, M. Boudart (Eds.), Hydrotreating catalysis, Catalysis Science and Technology, vol. 11, Springer, Berlin, 1996.
[7] D.D. Whitehurst, T. Isoda, I. Mochida, Adv. Catal. 42 (1998) 345.
[8] T. Kabe, A. Ishihara, W. Qian, Hydrodesulfurization and Hydrodenitrogenation, Chemistry and Engineering, Kodansha, Viley-VCE, 1999.
[9] M.J. Girgis, B.C. Gates, Ind. Eng. Chem. 30 (1991) 2021.
[10] R. Prins, V.H.J. de Beer, G.A. Somorjai, Catal. Rev. Sci. Eng. 31 (1989) 1.
[11] C. Song, X. Ma, Appl. Catal. B: Environ. 41 (2003) 207.
[12] S. Eijsbouts, Appl. Catal. A: Gen. 158 (1997) 53.
[13] H. Topsøe, B.S. Clausen, Catal. Rev. Sci. Eng. 26 (1984) 395.
[14] S.M.A.M. Bouwens, F.B.M. van Zon, M.P. van Dijk, A.M. van der Kraan, V.H.J. de Beer, J.A.R. van Veen, D.C. Koningsberger, J. Catal. 146 (1994) 375.
[15] B.S. Clausen, H. Topsøe, R. Candia, J. Villadsen, B. Lengeler, J. Als-Nielsen, F. Christensen, J. Phys. Chem. 85 (1982) 3868.
[16] B.S. Clausen, B. Lengeler, H. Topsøe, R. Candia, in: K.O. Hodgson, B. Hedman, J.E. Penner-Hahn (Eds.), EXAFS and Near Edge Structure II, Springer, Berlin, 1984, p. 181.
[17] M. Boudart, J.S. Arrieta, B.R. Dalla Betta, J. Am. Chem. Soc. 105 (1983) 6501.

[18] F.E. Massoth, Characterization of Molybdena Catalysts, Adv. Catal. 27 (1978) 265.
[19] K. Segawa, W.K. Hall, J. Catal. 77 (1982) 221.
[20] N.Y. Topsøe, H. Topsøe, J. Catal. 75 (1982) 354.
[21] S.S. Pollack, J.V. Sanders, R.E. Tischer, Appl. Catal. 8 (1983) 383.
[22] F. Delannay, Appl. Catal. 16 (1985) 135.
[23] R. Sharma, H.D. Burtron, Catal. Lett. 17 (1993) 363.
[24] J. Grimblot, P. Dufresne, L. Gengembre, J.P. Bonnelle, Bull. Soc. Chim. Belg. 90 (1981) 1261.
[25] C. Pophal, F. Kameda, K. Hoshino, S. Yoshinaka, K. Segawa, Catal. Today 39 (1997) 21.
[26] S. Yoshinaka, K. Segawa, Catal. Today 45 (1998) 293.
[27] K. Segawa, K. Takahashi, S. Satoh, Catal. Today 63 (2000) 123.
[28] K. Takahashi, Y. Saih, K. Segawa, Stud. Surf. Sci. Catal. 145 (2002) 311.
[29] Y. Saih, K. Segawa, Catal. Today 86 (2003) 61.
[30] Y. Saih, K. Segawa, Catal. Surv. Asia 7 (4) (2003) 235.
[31] Y. Saih, K. Segawa, Appl. Catal. A: Gen. 353 (2009) 258.
[32] K. Segawa, Q. Gao, C.T. Williams, Prepr. Pap. -Am. Chem. Soc., Div. Pet. Chem. 54 (2) (2009) 49.
[33] H. Wang, R. Prins, J. Catal. 264 (2009) 31.
[34] T. Kabe, A. Ishihara, Q. Zhang, Appl. Catal. A: Gen. 97 (1993) L1.
[35] J.H. Kim, X. Ma, C. Song, Y.K. Lee, S.T. Oyama, Energy Fuels 19 (2005) 353.
[36] Y. Saih, M. Nagata, T. Funamoto, Y. Masuyama, K. Segawa, Appl. Catal. A: Gen. 295 (2005) 11.
[37] T. Weber, J.C. Muijsers, J.H.M.C. van Wolput, C.P.J. Verhagen, J.W. Niemantsverdriet, J. Phys. Chem. 100 (1996) 14144.
[38] S. Eijsbouts, L.C.A. van den Oetelaar, R.R. van Puijenbroek, J. Catal. 229 (2005) 352.